Chapter 3

SCANNING TUNNELING MICROSCOPY STUDIES OF MONOLAYER TEMPLATES: ALKYLTHIOETHERS AND ALKYLETHERS

3.1 Overview

Scanning tunneling microscopy has been used to determine the molecular ordering in stable, ordered monolayers formed from long-chain normal and substituted alkanes in solution on highly oriented pyrolytic graphite surfaces. Monolayers were initially formed using an overlying solution of either a symmetrical dialkylthioether or a symmetrical dialkylether. Initially pure thioether solutions were then changed to nearly pure solutions of the identical chain-length ether, and vice versa. The direct application of a pure solution of long-chain symmetrical ethers onto graphite produced a lamellate monolayer within which the individual molecular axes were oriented at an angle of ~ 65° to the lamellar axes. In contrast, a pure solution of long-chain symmetrical thioethers on graphite produced a monolayer within which the molecular axes were oriented perpendicular to the lamellar axes. When ethers were gradually added to solutions overlying pure thioether monolayers, the ethers substituted into the existing monolayer structure. Thus the ether molecules could be forced to orient in the perpendicular thioether-like manner through the use of a thioether template monolayer. Continued addition of ethers to the solution ultimately produced a nearly pure ether monolayer that retained the orientation of the thioether monolayer template. However, a monolayer of thioether molecules formed by gradual substitution into an ether monolayer did not retain the 65° orientation typical of dialkylethers, but exhibited the 90° orientation typical of dialkylthioether monolayers. The thioethers and ethers were easily distinguished in images of mixed monolayers, allowing both an analysis of the distribution of the molecules within the mixed monolayers and a comparison of the monolayer compositions with those of the overlying solutions. Substitution of molecules into the template monolayer did not proceed randomly; instead, a molecule within a

monolayer was more likely to be replaced by a molecule in the overlying solution if it was located next to a molecule that had already been replaced.

3.2 Introduction

Long-chain normal and substituted alkanes in solution spontaneously adsorb onto a number of surfaces, including graphite, molybdenum disulfide, and tungsten disulfide.[1] This physisorption process results in the formation of stable, highly ordered monolayers at the solid–liquid interface, and has found relevance in the fields of lubrication, separation, adhesion, catalysis, crystallization, and corrosion-resistance. When an atomically flat surface such as highly oriented pyrolytic graphite (HOPG) is used as a substrate, a scanning tunneling microscope (STM) can be used to obtain images of the adsorbed monolayers.[2–4] Images obtained using this method often exhibit atomic-scale resolution, and commonly reveal a single ordered monolayer domain covering a relatively large area of the surface. Physisorbed monolayers represent a route to the spontaneous assembly of highly ordered surface structures with nanometer-scale features, and are thus of particular interest for surface patterning.

The orientation of molecules within a physisorbed monolayer is determined by the shape of the molecules and by the interactions between functional groups.[5–8] The surface structures of such physisorbed monolayers generally result in simple two-dimensional patterns. Production of more complex patterns requires the use of overlying solutions that contain a mixture of molecules, or the use of solutions of molecules that have elaborate or chiral structures.[9–15]

In an alternate approach, we recently reported that a monolayer of long-chain normal alkanes can act as a template for an ether monolayer.[16] The templating approach allows the production of a monolayer composed of molecules that have been forced to assume an atypical orientation. The direct application of a pure solution of symmetrical long-chain alkylethers or long-chain alkylthioethers onto a clean HOPG surface results in the formation of a lamellate monolayer; however, the ether molecules lie with their molecular

axes at an angle of ~ 65° to the lamellar axes, while the thioethers lie with their molecular axes perpendicular to the lamellar axes.[16–19] Interestingly, an ether monolayer composed of molecules oriented in the manner typical of alkanes can be produced through the use of an alkane monolayer template.[16] When the HOPG surface is first covered by a monolayer of the normal alkane and the composition of the overlying solution is subsequently changed to favor the symmetrical ether of the same chain length, the ether molecules replace the alkanes while retaining the structure of the alkane monolayer template. Although these earlier studies readily allowed observation of the monolayer templating effect, alkanes and ethers could not confidently be distinguished in the mixed monolayers, due to insufficient functional group contrast in typical STM images of such systems.

In this work, we report the results of a series of experiments involving monolayers of symmetrical alkylthioethers and symmetrical alkylethers. The lamellate monolayers formed on HOPG by pure solutions of symmetrical alkylthioethers are similar to those formed by normal alkanes, in that the thioether molecules lie with their molecular axes perpendicular to the lamellar axes. However, ether and thioether functional groups are easily distinguished in STM images, with the oxygen atom of the ether functionality appearing as a dark, low-contrast region, whereas the sulfur atom in an alkylthioether appears as a bright, high-contrast region. The contrast between the oxygen and sulfur atoms is substantially greater than the contrast observed between alkanes and alkylethers, enabling direct and confident determination of the composition of the mixed monolayers in STM images.[19,21] By extending the study of monolayer templates to include dialkylthioethers, we have been able to monitor the progress of template replacement, to analyze the distribution of molecules within mixed monolayers, and to compare the monolayer composition with that of the overlying solution.

3.3 Experimental Details

Experiments were performed using length-matched (in their all *trans*- configuration) pairs of the following symmetrical dialkylthioethers and dialkylethers: di-*n*-tetradecylsulfide and

di-*n*-tetradecylether; di-*n*-hexadecylsulfide and di-*n*-hexadecylether; di-*n*-octadecylsulfide and di-*n*-octadecylether (all from TCI America, > 95% purity). Table 3.1 lists the chemical formulas and abbreviations used herein for these six compounds. Solutions containing each of these compounds were prepared in phenyloctane (Acros, 99% pure). Phenyloctane is commonly used as a solvent in studies of physisorbed monolayers because it does not form a monolayer on HOPG, and thus does not compete with the formation of monolayers by the dissolved species. The thioethers and ethers used in this study are sparingly soluble in phenyloctane. The solutions were filtered before use and were approximately saturated at room temperature. The concentrations of the solutions were determined using an HP 6890 gas chromatograph equipped with a flame ionization detector, with 1-bromohexadecane (Aldrich) used as an internal standard. The concentrations of the pure solutions were as follows: E29, 75 mM; E33, 71 mM; E37, 4.8 mM; S29, 61 mM; S33, 11 mM; S37, 3.5 mM. The ethers were more soluble than the thioethers, and shorter molecules were more soluble than longer ones. Four or more mixed solutions were prepared for each of the three length-matched pairs of thioethers and ethers. The mixed solutions were prepared by mixing volumes of the matched ether and sulfide solutions in ratios of 80:20, 60:40, 40:60, and 20:80.

HOPG (Grade SPI-1 from Structure Probe Inc.) was freshly cleaved and secured in a cell that could contain liquids while still allowing STM imaging. The surface was then imaged under ambient conditions using a fresh, mechanically cut 80:20 Pt/Ir tip. Images were collected using a Digital Instruments (Veeco) Nanoscope III STM controlled by Nanoscope software version 5.12r2. Each image consisted of 512 sample lines. A real-time plane-fitting function was applied to the images during scanning, but no further image corrections were performed. After images of the bare HOPG were obtained at atomic-scale resolution, a 15 μL drop of a pure thioether or ether solution was placed onto the graphite surface. After ~ 30–45 min, the resulting monolayer was imaged with the STM. Imaging conditions were typically 1200 mV sample bias, with a constant current of 200 pA. A 5 μL drop of the mixed solution that contained the next lower concentration of the species already present on the surface was then added to the cell. For example, after imaging a

monolayer formed from a pure S29 solution, 5 μL of the 80:20 S29/E29 mixture was added to the cell. After allowing ~ 30–45 min for equilibration of the mixture, the resulting monolayer was then observed with the STM. Once images were collected, 5 μL of liquid were removed from the cell, and the liquid was replaced with the same volume of a mixed solution. The relative concentration of the mixture component that was initially present on the surface and in the initial overlying solution was gradually reduced by removing liquid from the cell, and replacing the volume removed with equal volumes of mixed solutions that contained successively lower amounts of the first component of the length-matched pair. The process was continued until the solution composition greatly favored the component that was not initially present on the surface. Solutions containing only the second mixture component were used in the final repetitions of an experiment, to further increase the concentration of the second mixture component in the solution above the HOPG surface. In the example of S29 and E29 given above, after gradually reducing the concentration of S29 in the overlying solution, a few portions of pure E29 solution were added to the cell, to further eliminate the thioether from the system. Tunneling tips were not changed during an experiment, to avoid mechanically disturbing the monolayers. An internal standard was added to the portions of liquid removed from the cell during each experiment, and gas chromatography was used to monitor the composition of the overlying solution by analysis of such samples. These experimental procedures were conducted multiple times, starting with overlying solutions of each of the three thioethers and each of the three ethers.

Well-resolved STM images of physisorbed monolayers were obtained throughout the course of these experiments. The effects of thermal drift were minimal, and the STM images thus allowed determination of the orientation of the molecules within the monolayers, as measured using tools available in the Nanoscope III software. The compositions of the monolayers, and the distributions of each species within the mixed monolayers, were then analyzed using computer software that was written for these purposes. This software superimposed a scaled grid upon each STM image. The grid was then adjusted by the user to correspond to the orientation of the molecules in the monolayer

image, such that each cell of the grid corresponded to a single molecule in the STM image. The user then selected a threshold contrast level, which the software then compared to the average image contrast level over a region in the center of each grid cell. These compared regions thus corresponded to the centers of the molecules, where either a dark oxygen atom or a bright sulfur atom was present. Molecules with centers that had average contrast values higher than the threshold were identified as thioethers, and those that had lower contrasts than the threshold were identified as ethers. The results of the analysis were then overlaid on the image, allowing the user to confirm that the program had correctly performed the molecular identification function. The number and location of molecules of each species within the image were recorded by the software, and the observed distribution of molecules was then compared to statistics produced by 10,000 computer-generated random distributions calculated for the same monolayer structure and composition. These random distributions were then used to calculate the likelihood of finding each length of a cluster within the monolayer in which adjacent molecules were of the same species. The primary role of the software was to assist in counting the large number of molecules in each of a large number of images, and to record both the numbers of molecules and their positions within each monolayer. The output of the program was easily monitored and verified by the user.

3.4 Results

Figure 3.1 and Figure 3.2 show representative STM images of monolayers formed at the interface between HOPG and a solution of either a thioether or an ether. Alkylthioether molecules within monolayers formed in the absence of an alkylether were observed to lie with their molecular axes perpendicular to their lamellar axes. In contrast, alkylethers within monolayers formed in the absence of an alkylthioether were observed to lie with their molecular axes at an angle of ~ 65° with respect to their lamellar axes.[16–19] Two cases of structural polymorphism relevant to our work have been reported, one each for alkylthioether and alkylether monolayers. Fukumura et al. reported a second monolayer structure for thioether S37, with molecules positioned with their axes at an angle of ~ 60°

with respect to the lamellar axes, similar to the orientation of alkylethers.[20] Padowitz et al. observed for a monolayer of di-*n*-docosylether, $CH_3(CH_2)_{21}O(CH_2)_{21}CH_3$, both the typical 65° structure and a perpendicular structure.[19] Di-*n*-docosylether has a significantly longer chain length than the ethers used in this study. These authors believed that the perpendicular structure was promoted by the scanning motion of the STM tip and reported that the structure was unstable.[19] We did not observe either of these polymorphisms during our study. Dialkylthioether monolayers appeared to form more readily than monolayers of the identical chain-length ether. This observation suggests that the adsorption of dialkylthioethers onto graphite is more favorable than adsorption of the comparable dialkylether. Monolayers formed most readily for the longest chain-length molecules, which is consistent with expectations and with the reported thermodynamic data for adsorption of hydrocarbons on graphite.[22]

After mixtures of length-matched ether and thioether molecules were added to the solutions overlying pure monolayers, the newly introduced molecular species incorporated into the existing monolayer domains (Figure 3.3). Segregation of the two mixed species into separate domains was not observed. The perpendicular orientation of molecules displayed by pure dialkylthioether monolayers was retained even as the molecules in these monolayers were replaced by the length-matched alkylether and as the surface mole fraction of the alkylether exceeded 0.90. In fact, ether molecules within monolayers formed from a thioether template retained the perpendicular orientation even after the monolayers were left undisturbed for 24–48 h (Figure 3.3d). In contrast, the orientation of molecules exhibited by a pure dialkylether monolayer was not retained when dialkylthioether molecules were added to the overlying solution (Figure 3.3b). The structure of the dialkylether monolayer was consistently lost and replaced by the perpendicular structure typical of the dialkylthioether as the mole fraction of thioether in the overlying solution and on the surface approached 0.10. Therefore, dialkylthioether monolayers were observed to act as templates for dialkylether monolayers, but dialkylether monolayers did not act as templates for dialkylthioether monolayers.

The contrast between the alkylether and alkylthioether molecules in the STM images allowed the two molecule types to be distinguished. Figure 3.4a depicts an example of the over 100 high-quality images that were obtained throughout the set of experiments and analyzed using the image analysis software. An example image analysis is shown in Figure 3.4b. For the example shown in Figure 3.4b, single ether molecules, and clusters of as many as six ethers, are clearly visible in the predominately thioether monolayer. The distribution of ethers and thioethers within each mixed monolayer image was compared to the average of 10,000 computer-generated random distributions for the identical monolayer size, orientation, and composition (Figure 3.4c). The observed molecular distributions were consistently well outside of the standard deviations of the random distributions, and were consistently shifted toward larger cluster sizes. This indicates that, within a mixed monolayer lamella, the probability of a species having an identical species as a neighbor, i.e., a thioether next to a thioether or an ether next to an ether, was much greater than could be attributed to random chance.

The image analysis software also recorded the molecular composition found in each mixed monolayer image. These values were then compared to the measured composition of the overlying solution that was in contact with the HOPG when the image was obtained (Figure 3.5). When the mole fraction of thioether in solution was 0.3–0.9, the mole fraction of thioethers in a mixed monolayer exceeded that of the overlying solution. This behavior was independent of the direction in which this range of solution mixture compositions was approached. The measured surface excess of thioethers was greatest at the low end of this range of solution composition. These results are consistent with the preferential adsorption onto HOPG of thioethers relative to ethers.

3.5 Discussion

The results of this series of experiments are consistent with those obtained earlier using long-chain alkanes and symmetrical dialkylethers.[16] In the present work, the dialkylthioether monolayers acted as a template when they were replaced by dialkylethers, with the thioether template forcing the alkylethers to lie with their molecular axes

perpendicular to the lamellar axes. In stark contrast with the reported di-*n*-docosylether polymorphism, the templated alkylether monolayers were highly stable and the structure did not preferentially align with the scanning motion of the STM tip. The alkylether monolayers, however, did not act as templates during the replacement of the ethers by the thioethers.

Two cases of structural polymorphism relevant to our work have been reported. For the S37 thioether, a second monolayer structure has been observed, in which the molecules were positioned with their axes at an angle of ~ 60° with respect to the lamellar axes, similar to the orientation of alkylethers.[20] For a monolayer of di-*n*-docosylether, $CH_3(CH_2)_{21}O(CH_2)_{21}CH_3$, the typical 65° structure and a perpendicular structure have been observed.[19] Di-*n*-docosylether has a significantly longer chain length than the ethers used in this study. The authors of that work believed that the perpendicular structure was promoted by the scanning motion of the STM tip and reported that the structure was unstable.[19] We did not observe either of these polymorphisms in the monolayers investigated in our study. In contrast with the reported di-*n*-docosylether polymorphism, the templated alkylether monolayers were highly stable and the structure did not preferentially align with the scanning motion of the STM tip.

For alkanes, adjacent molecules within a lamellar domain experience favorable van der Waals interactions, and the total strength of these interactions is proportional to the length of the alkane chain.[23] These interactions are thus expected to stabilize the formation of the structure in the physisorbed alkane monolayers. Such interactions are maximized when the molecules line up and lie with their axes perpendicular to the lamellar axes.[24] Assuming that the observed thioether structures indicate the minimum energy overlayer structures for these molecules, the STM data obtained herein thus suggest that analogous interactions are involved in determining the structure of the thioether monolayers. For ethers, the difference of 0.89 P between the electronegativities of oxygen (2.55 P) and carbon (3.44 P) implies the presence of a partial negative charge on the oxygen atom. In the structure observed for monolayers of alkylethers, neighboring molecules are offset by two carbon

atoms, resulting in the 65° angle between the axes (Figure 3.1b). Assuming that the structure observed for the pure untemplated ethers is the most stable structure for the molecules investigated implies that both favorable van der Waals interactions and unfavorable electrostatic repulsions are important in determining the structure of the untemplated pure ether overlayers. The concomitant decrease in the number of van der Waals interactions in the ether monolayers having the 65° angle between the axes, along with effects of polarizability on the strength of adsorption of ethers versus thioethers, correlates with the weaker adsorption observed for an ether relative to that of the identical chain-length alkane or thioether.

When dialkylether molecules are forced by a template to conform to the orientation of an alkane or dialkylthioether monolayer, the energy increase due to adoption of the higher-energy (perpendicular) structure for these ethers is expected to be partially offset by the addition of favorable van der Waals interactions between adjacent molecules in a lamella. However, when dialkylthioether molecules replace molecules of a dialkylether monolayer, the 65° angle between the molecular and lamellar axes causes the loss of the potential van der Waals interactions without providing sufficient offsetting favorable interactions. These expectations are therefore consistent with the observation that the alkylether monolayers did not act as templates for alkylthioether monolayers. Calorimetric studies of the adsorption of alkylthioethers and alkylethers onto HOPG could provide further information on the relative contributions of the surface adsorption energies and intermolecular electrostatic repulsion energies that result in the 65° orientation observed for monolayers of pure alkylethers, and computational methods may provide further insight into the factors that control the packing in templated and untemplated alkylether and alkylthioether monolayers.

The concentration of alkylethers in solutions overlying mixed monolayers consistently exceeded the surface alkylether concentration until the mole fraction of alkylethers in the overlying solution exceeded 0.70, as can be seen in Figure 3.5. The differences between the compositions of the overlying solutions and of the mixed monolayers indicate that the

thioethers are more strongly adsorbed onto HOPG than the ethers. This behavior is consistent with our observations that thioether monolayers form more readily than monolayers of the identical chain-length ether, and with the expectation that the oxygen–oxygen interaction is repulsive. The preference for adsorption of thioethers was observed to be independent of the species that was initially present on the surface and in the overlying solution. Alkylether monolayers did not act as templates for the alkylthioethers, and data collection for experiments that began with alkylether monolayers was ended once the monolayer structure was observed to have completed the change to the structure characteristic of thioethers. Therefore, the data presented in Figure 3.5 were collected during the templating process and analogous data for mixed, but not templated, monolayers were not collected.

We previously proposed that replacement of molecules within a monolayer proceeded via filling openings left in the monolayer by molecules that had desorbed from the surface.[16] Although additional factors, such as the relative concentrations of the two species in the overlying solution and their relative energies of adsorption, are expected to affect the details of the monolayer substitution process, the relative rates of desorption from the monolayer will dominate the template substitution. Desorption from these monolayers is an activated process,[25] and the ease of removing a molecule from the surface depends upon the strength of its interactions with its neighbors. For example, since the formation of the observed ether overlayers is presumed to be less favored thermodynamically than the formation of the observed thioether monolayers, an ether molecule that has two ether neighbors would be expected to be more readily removed from a monolayer than an ether molecule that has two thioether neighbors. However, once an individual molecule is removed from a monolayer, stabilizing interactions are lost by the molecules that are adjacent to the new vacant site. The probability that these former neighbors will also be removed from the surface is therefore increased significantly, until the vacancy is filled by a molecule from the overlying solution. This process would result in non-random replacement of molecules in a template monolayer.

In our previous work, we estimated that the non-optimal interactions in ether monolayers resulted in a stability loss of ~ 8 kcal mol^{-1} in ether monolayers on HOPG relative to monolayers formed from the identical chain-length alkane on HOPG. The adsorption of a long-chain alkane onto graphite is believed to be primarily driven by van der Waals interactions between neighboring molecules, in accord with the observation that the heat of adsorption for long-chain alkanes increases linearly with increasing chain length.[22] Thus, if the energy of adsorption arises from stabilization of a molecule by two neighbors, the stability loss that a molecule in a monolayer would experience as the result of the removal of one of its neighbors can be estimated to be about one-half of that value. The heats of adsorption onto graphite for the molecules used in this study have not been reported; however, we expect the average value for these molecules to be comparable to the heat of adsorption for n-dotriacontane, which has been measured to be ~ 35 kcal mol^{-1}.[1,22] The loss of such interactions can thus be expected to dominate the monolayer substitution process. Others have suggested that the replacement of molecules in a monolayer does not proceed randomly.[19] The distribution analyses described herein for mixed monolayers, and illustrated in Figure 3.4c, support this hypothesis. Our results are therefore consistent with a process in which the replacement of a molecule on the surface greatly increases the probability that its neighbors will also be replaced.

3.6 Conclusions

When molecules in monolayers of symmetrical dialkylthioethers are replaced by molecules of the identical chain-length symmetrical dialkylether, the structure of the dialkylthioether monolayer is retained. This is not the case when molecules in monolayers of dialkylethers are replaced by dialkylthioethers. These results supplement our earlier work with normal alkanes and alkylethers, through the additional ability to distinguish between the thioether and ether molecules in the STM images of mixed monolayers. This ability has allowed confirmation that dialkylthioethers are more strongly physisorbed than the identical chain-length dialkylether, and that the replacement of molecules in a monolayer does not proceed randomly. Calorimetric studies of the adsorption of alkylthioethers and alkylethers onto

HOPG would provide an accurate measure of the contribution of the electrostatic repulsion that produces the 65° orientation in monolayers of alkylethers, and computational methods may provide further insight into packing in templated alkylether monolayers. Additional work with mixtures that contain molecules having differing lengths and other functional groups may allow monolayer templates to serve as a practical tool for controlling the structure of physisorbed monolayers.

Table 3.1 Molecular Names, Formulas, and Abbreviations

Name	Formula	Abbreviation
di-*n*-tetradecylsulfide	$CH_3(CH_2)_{13}S(CH_2)_{13}CH_3$	S29
di-*n*-tetradecylether	$CH_3(CH_2)_{13}O(CH_2)_{13}CH_3$	E29
di-*n*-hexadecylsulfide	$CH_3(CH_2)_{15}S(CH_2)_{15}CH_3$	S33
di-*n*-hexadecylether	$CH_3(CH_2)_{15}O(CH_2)_{15}CH_3$	E33
di-*n*-octadecylsulfide	$CH_3(CH_2)_{17}S(CH_2)_{17}CH_3$	S37
di-*n*-octadecylether	$CH_3(CH_2)_{17}O(CH_2)_{17}CH_3$	E37

Figure 3.1 STM Image and Model of a Monolayer of Hexadecylether

(a) A constant-current mode STM image of di-*n*-hexadecylether, $CH_3(CH_2)_{15}O(CH_2)_{15}CH_3$, on HOPG. The imaging conditions were I = 250 pA, V_{bias} = 1200 mV, and a scan rate of 30.5 Hz.

(b) A model of di-*n*-hexadecylether molecules on HOPG. The molecular axis is shown with a dashed arrow, and the lamellar axis is shown with a solid arrow. The angle between the two axes is 65°.

Figure 3.1 STM Image and Model of a Monolayer of Hexadecylether

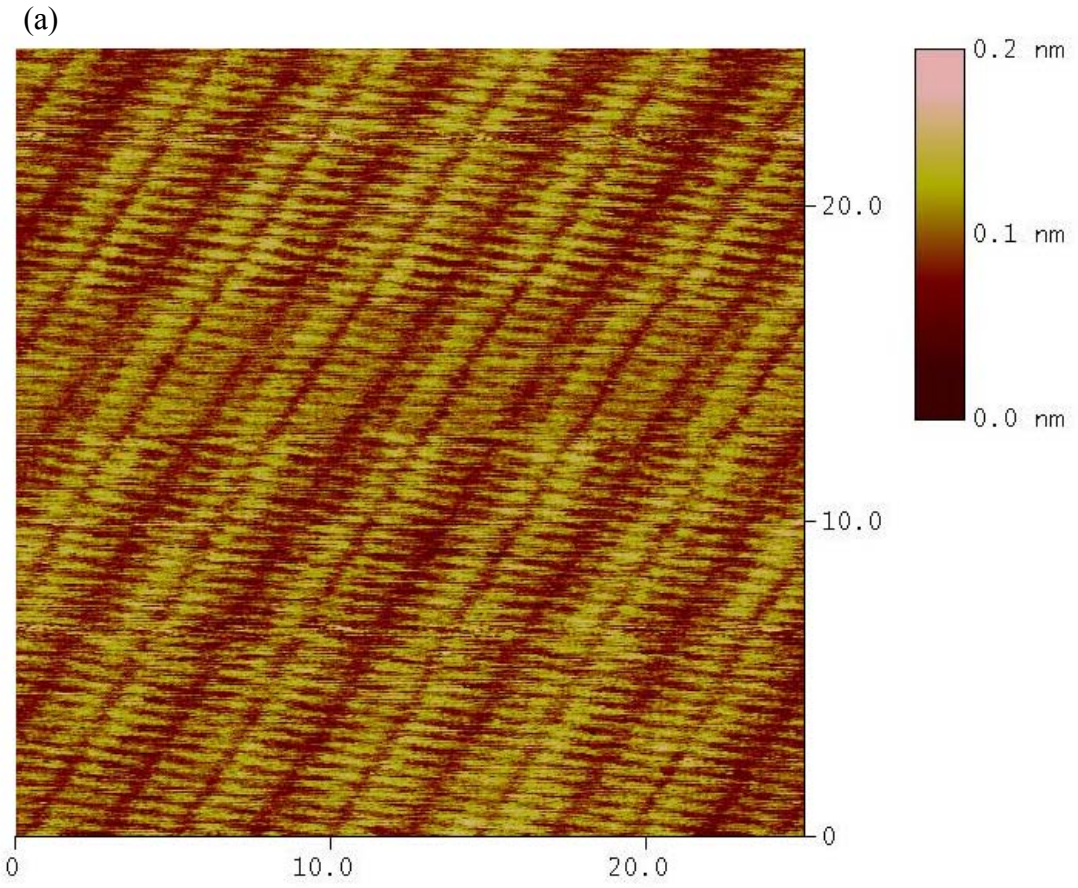

Figure 3.2 STM Image and Model of a Monolayer of Hexadecylsulfide

(a) A constant height mode STM image of di-*n*-hexadecylsulfide, $CH_3(CH_2)_{15}S(CH_2)_{15}CH_3$, on HOPG. The imaging conditions were I = 200 pA, V_{bias} = 1200 mV, and scan rate = 30.5 Hz.

(b) A model of di-*n*-hexadecylsulfide molecules on HOPG. The molecular axis is perpendicular to the lamellar axis.

Figure 3.2 STM Image and Model of a Monolayer of Hexadecylsulfide

(a)

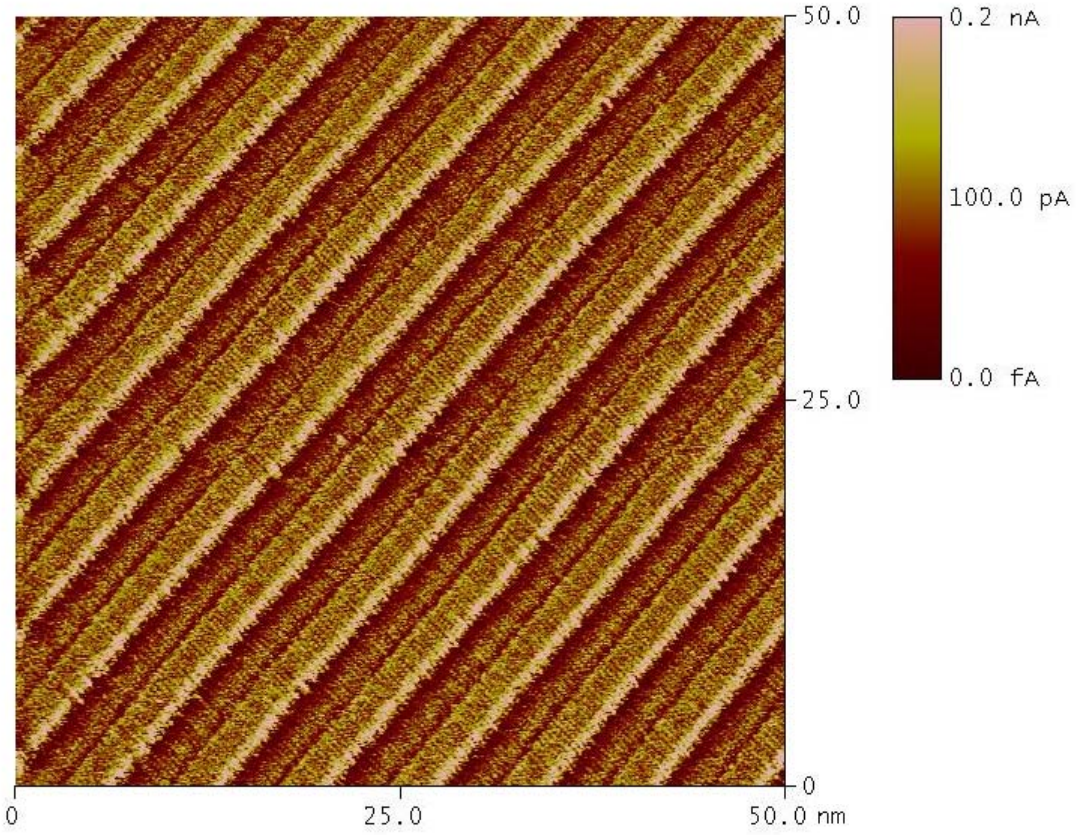

(b)

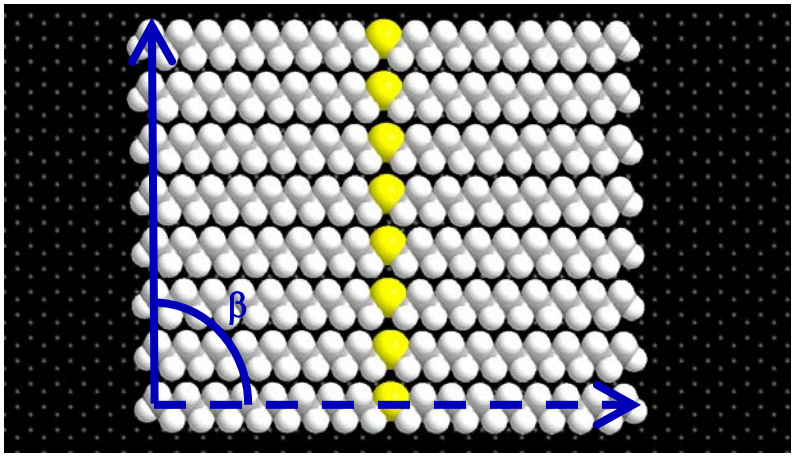

Figure 3.3 STM Images of Mixed Monolayers of Alkylthioethers and Alkylethers

(a) A constant-current STM image of the mixed monolayer obtained after addition of di-*n*-hexadecylsulfide to a di-*n*-hexadecylether solution. The white lines mark four molecules, and two thioether molecules are indicated by arrows. Imaging conditions: I = 200 pA, V_{bias} = 1100 mV, scan rate = 30.5 Hz

(b) The monolayer after further addition of di-*n*-hexadecylsulfide. Two lamellae are indicated by arrows. The molecules lie with their axes perpendicular to the lamellar axes, thus the orientation of the ether template monolayer has been lost. Imaging conditions: I = 200 pA, V_{bias} = 1100 mV, scan rate = 20.3 Hz

(c) An STM image obtained after di-*n*-octadecylether was added to a di-*n*-octadecylsulfide solution. Four molecules are marked with white lines, and arrows indicate ethers that have incorporated into the thioether layer. Imaging conditions: I = 200 pA, V_{bias} = 1200 mV, scan rate = 30.5 Hz

(d) The monolayer after further addition of di-*n*-octadecylether. The ether molecules lie with their axes perpendicular to the lamellar axes, retaining the orientation of the thioether monolayer template. Several thioether molecules have remained in the monolayer and can be distinguished by bright spots in their centers. Two thioether molecules are indicated by arrows. Imaging conditions: I = 200 pA, V_{bias} = 1100 mV, scan rate = 30.5 Hz

Figure 3.3 STM Images of Mixed Monolayers of Alkylthioethers and Alkylethers

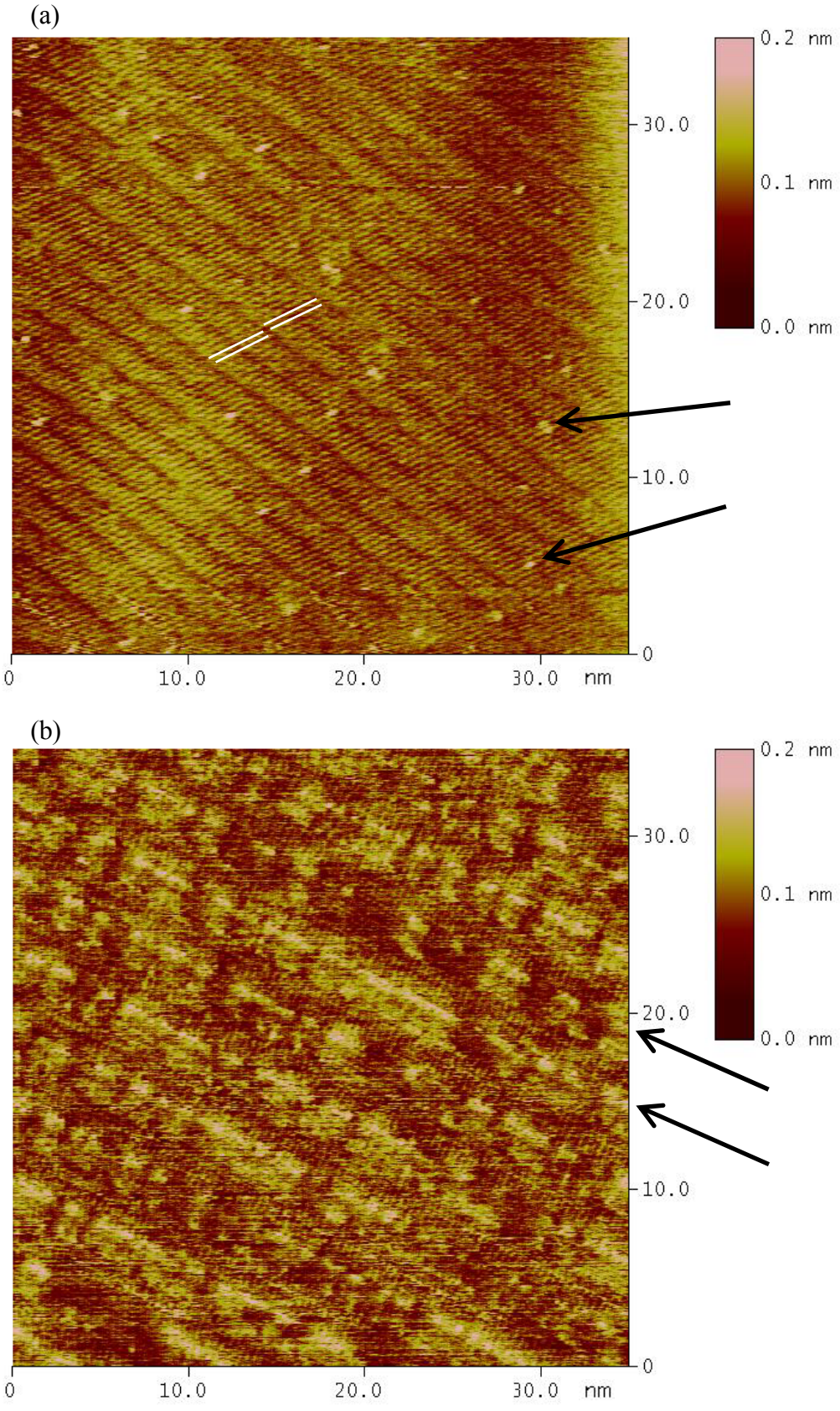

Figure 3.3 STM Images of Mixed Monolayers of Alkylthioethers and Alkylethers

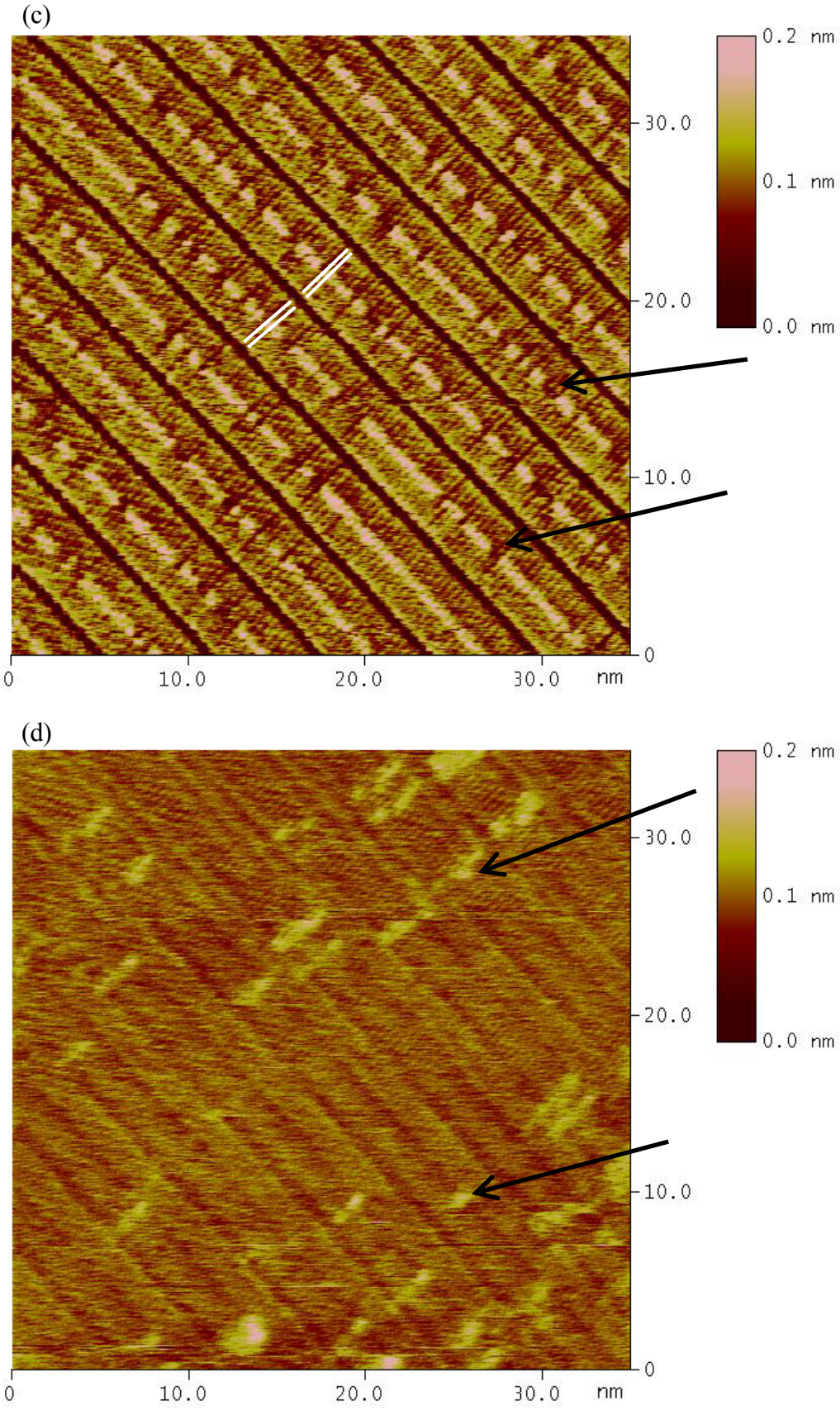

Figure 3.4 Mixed Monolayer Analysis Software

(a) An STM image of a mixed monolayer of di-*n*-octadecylsulfide and di-*n*-octadecylether. The imaging conditions were I = 200 pA, V_{bias} = 1200 mV, and scan rate = 30.5 Hz.

(b) A grid has been superimposed upon the image by the analysis software, and the center of each ether molecule has been marked with a black dot. The largest cluster of ethers in the image contains six molecules.

(c) A comparison of the average observed distribution of ethers within mixed monolayers under identical conditions as panel (a) with the average values obtained for a random distribution of molecules. The solid bars represent the observed values and the cross-hatched bars represent the values for a calculated random distribution of molecules.

Figure 3.4 Mixed Monolayer Analysis Software

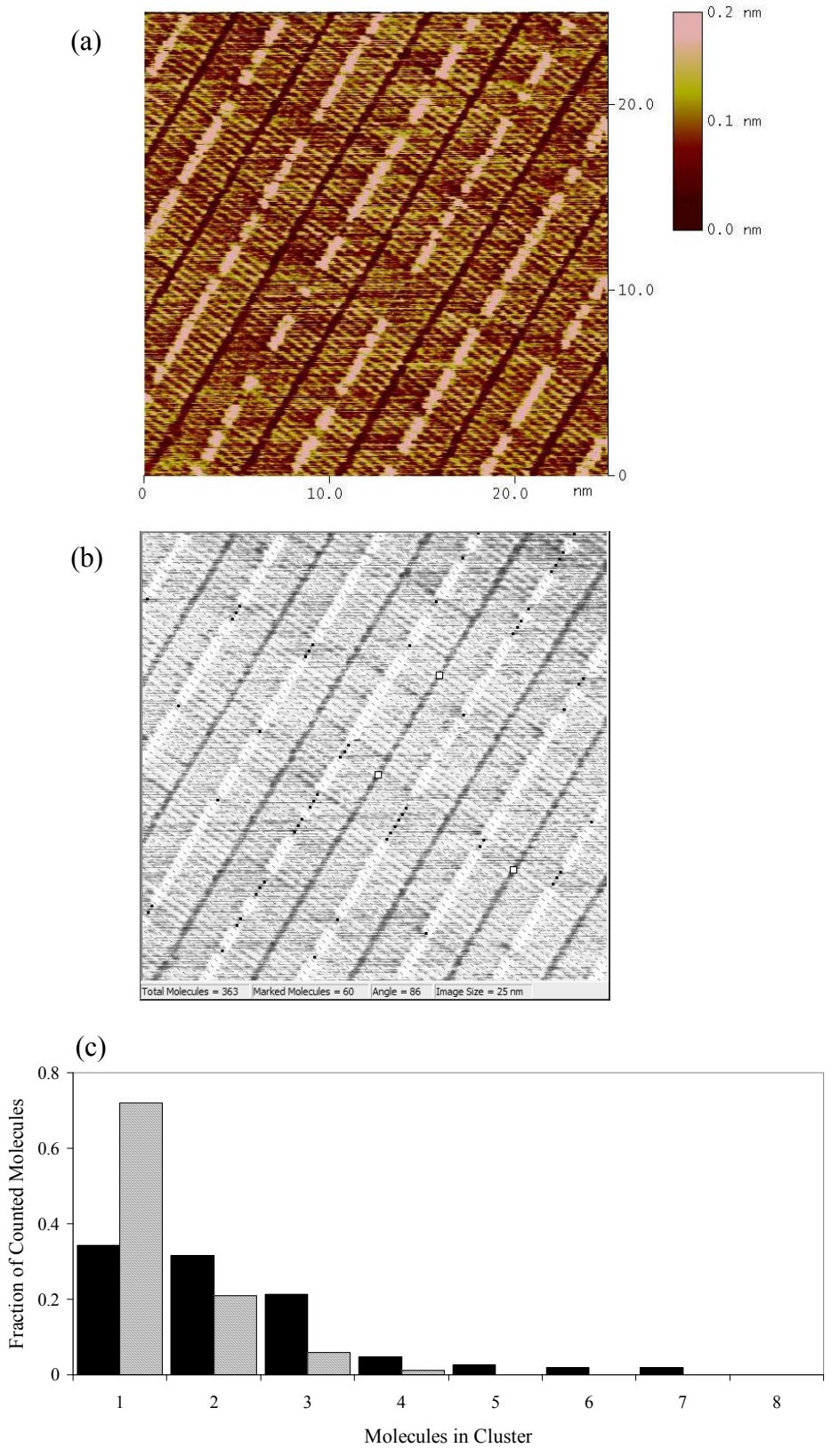

Figure 3.5 Solution Versus Surface Concentration

Comparison of the compositions of solutions overlying mixed alkylthioether/alkylether monolayers and the compositions of the monolayers as determined from STM images. The dashed line that indicates equal composition clearly does not fit the data. When the mole fraction of ether in the overlying solution, $\chi_{ether,soln}$, was less than 0.7, the ethers were underrepresented in the physisorbed monolayer as indicated by a smaller mole fraction of ether on the surface, $\chi_{ether,surf}$. The error bars represent one standard deviation.

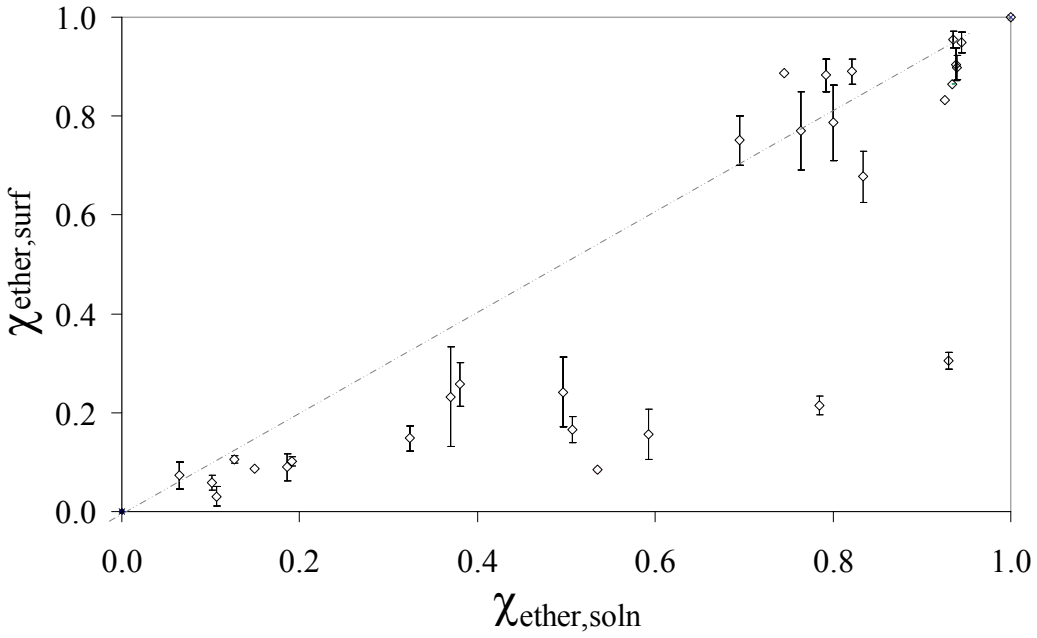

3.7 References

(1) Groszek, A. J. *Nature* **1964**, *204*, 680.

(2) McGonigal, G. C.; Bernhardt, R. H.; Thomson, D. J. *Appl. Phys. Lett.* **1990,** *57*, 28–30.

(3) Venkataraman, B.; Flynn, G. W.; Wilbur, J. L.; Folkers, J. P.; Whitesides, G. M. *J. Phys. Chem.* **1995,** *99*, 8684–8689.

(4) Rabe, J. P.; Buchholz, S. *Science* **1991,** *253*, 424–427.

(5) McGonigal, G. C.; Bernhardt, R. H.; Yeo, Y. H.; Thomson, D. J. *J. Vac. Sci. Technol., B* **1991,** *9*, 1107–1110.

(6) Freund, J. E.; Edelwirth, M.; Krobel, P.; Heckl, W. M. *Phys.l Rev. B* **1997,** *55*, 5394–5397.

(7) Gorman, C. B.; Touzov, I.; Miller, R. *Langmuir* **1998,** *14*, 3052–3061.

(8) Yin, S. X.; Wang, C.; Xu, Q. M.; Lei, S. B.; Wan, L. J.; Bai, C. L. *Chem. Phys. Lett.* **2001,** *348*, 321–328.

(9) Yablon, D. G.; Giancarlo, L. C.; Flynn, G. W. *J. Phys. Chem. B* **2000,** *104*, 7627–7635.

(10) Xie, Z. X.; Xu, X.; Mao, B. W.; Tanaka, K. *Langmuir* **2002,** *18*, 3113–3116.

(11) De Feyter, S.; Larsson, M.; Schuurmans, N.; Verkuijl, B.; Zoriniants, G.; Gesquiere, A.; Abdel-Mottaleb, M. M.; van Esch, J.; Feringa, B. L.; van Stam, J.; De Schryver, F. *Chem.—Eur. J.* **2003,** *9*, 1198–1206.

(12) Nanjo, H.; Qian, P.; Yokoyama, T.; Suzuki, T. M. *Jpn. J. Appl. Phys., Part 1* **2003,** *42*, 6560–6563.

(13) Wei, Y. H.; Kannappan, K.; Flynn, G. W.; Zimmt, M. B. *J. Am. Chem. Soc.* **2004,** *126*, 5318–5322.

(14) Plass, K. E.; Kim, K.; Matzger, A. J. *J. Am. Chem. Soc.* **2004,** *126*, 9042–9053.

(15) Tao, F.; Goswami, J.; Bernasek, S. L. *J. Phys. Chem. B* **2006,** *110*, 19562–19569.

(16) Papadantonakis, K. M.; Brunschwig, B. S.; Lewis, N. S. *Langmuir* **2008,** *24*, 857–861.

(17) Claypool, C. L.; Faglioni, F.; Goddard III, W. A.; Gray, H. B.; Lewis, N. S.; Marcus, R. A. *J. Phys. Chem. B* **1997,** *101*, 5978–5995.

(18) Nishino, T.; Buhlmann, P.; Ito, T.; Umezawa, Y. *Phys. Chem. Chem. Phys.* **2001,** *3*, 1867–1869.

(19) Padowitz, D. F.; Sada, D. M.; Kemer, E. L.; Dougan, M. L.; Xue, W. A. *J. Phys. Chem. B* **2002,** *106*, 593–598.

(20) Fukumura, H.; L-i, D.; Uji-i, H.; Nishio, S.; Sakai, H.; Ohuchi, A. *ChemPhysChem* **2005,** 6, (11), 2383–2388.

(21) Padowitz, D. F.; Messmore, B. W. *J. Phys. Chem. B* **2000,** *104*, 9943–9946.

(22) Groszek, A. J. *Nature* **1962,** *196*, 531–533.

(23) Kern, H. E.; Piechocki, A.; Brauer, U.; Findenegg, G.H. *Prog. Colloid Poly. Sci.* **1978,** *65*, 118–124.

(24) Claypool, C. L.; Faglioni, F.; Matzger, A. J.; Goddard III, W. A.; Lewis, N. S. *J. Phys. Chem. B* **1999,** *103*, 9690–9699.

(25) Paserba, K. R.; Gellman, A. J. *J. Chem. Phys.* **2001,** 115, 6737–6751.